



ORIGINAL PAPER

Dose to the skin in helical tomotherapy: Results of *in vivo* measurements with radiochromic films

Michele Avanzo ^{a,*}, Annalisa Drigo ^a, Stefano Ren Kaiser ^b,
Antonella Roggio ^c, Giovanna Sartor ^a, Paola Chiovati ^a,
Giovanni Franchin ^d, Maurizio Mascarin ^d, Elvira Capra ^a

^a Department of Medical Physics, IRCSS Centro di Riferimento Oncologico, via Franco Gallini 2, 33081 Aviano (PN), Italy

^b Department of Medical Physics, Fondazione Poliambulanza Istituto Ospedaliero, Brescia 25124, Italy

^c Department of Medical Physics, Veneto Institute of Oncology – IRCSS, Padua 35128, Italy

^d Department of Radiation Oncology, IRCSS Centro di Riferimento Oncologico, Aviano 33081, Italy

Received 2 August 2011; received in revised form 10 April 2012; accepted 14 April 2012

Available online 8 May 2012

KEYWORDS

Intensity modulated;
IMRT;
Skin dose;
In vivo dosimetry;
Helical tomotherapy;
Radiochromic films

Abstract *Purpose:* The aim of this study is to report results of measurements of dose to the skin *in vivo* with radiochromic EBT films in treatments with helical tomotherapy.

Methods and materials: *In vivo* measurements were performed by applying pieces of radiochromic films to the skin or to the inner side of thermoplastic mask before the treatment. The sites of treatment included scalp, brain, head and neck, cranio-spinal axis and lower limbs. Skin dosimetry was performed in a patient who experienced grade 3–4 acute side effects to the skin shortly after the first treatment sessions. For each patient we measured the setup errors using the daily MVCT acquired for image guidance of the treatment. EBT films were read with a flatbed Epson Expression scanner and images were processed with an in-house written routine.

Results: A total of 96 measurements of dose to the skin performed on 14 patients. The mean difference and standard error of the mean difference between measured and TPS-calculated dose was $-9.2\% \pm 2.6\%$ for all treatments, $-6.6\% \pm 2.6\%$ for head and neck treatments. These differences were statistically significant at the 0.05 significance level (*t*-Student test). Planned dose and dose range in the region of measurements were not correlated with dose discrepancy.

Conclusions: Radiochromic EBT films are suitable detectors for surface dose measurements in tomotherapy treatments. Results show that TPS overestimates dose to the skin measured with EBT radiochromic films. *In vivo* skin measurements with EBT films are a useful tool for quality

* Corresponding author. Tel.: +39 (0)434 659175.

E-mail address: mavanzo@cro.it (M. Avanzo).

assurance of tomotherapy treatments, as the treatment planning system may not give accurate dose values at the surface.

© 2012 Associazione Italiana di Fisica Medica. Published by Elsevier Ltd. All rights reserved.

Introduction

Intensity modulated radiation therapy (IMRT) has improved target coverage and sparing of organs at risk compared with 3D conformal radiotherapy (3D-CRT) and is now, for many pathologies, the treatment of choice [1].

Clinical side effects to superficial structures are a major concern with radiotherapy patients, particularly in IMRT. Toxicity to the skin and mucosa can happen more frequently if chemotherapy is administered in combination with radiation treatment [2]. Clinical side effects to superficial structures in radiotherapy typically occur in 2–3 weeks after the beginning of the radiation treatment and may cause, if they are not tolerated by the patient, a treatment break [3].

Incidences of toxicities to superficial structures, such as dermatitis and alopecia have been observed with IMRT treatments [4–6]. In a study on IMRT of oropharyngeal cancer the majority of patients developed skin toxicity or acute mucosal effects of grade 3 or 4 [6]. Scalp alopecia and anterior mucositis are associated with occipital scalp dose greater than 30 Gy and anterior mandible dose greater than 34 Gy [4]. Therefore it is recommended to draw skin as a sensitive structure and reduce dose to the skin in optimization of the IMRT plan [5]. The occurrence of complications in superficial structures as skin and mucosa in IMRT is possibly related to the increased number of tangential beams compared with 3D-CRT, resulting in more non-target tissues irradiated [4]. The dose to the skin could be higher in IMRT than in 3D-CRT also because, during the inverse planning, it is required to cover the PTV with the prescribed dose even in areas where build-up effect occurs [7].

Helical tomotherapy (Hi-Art II Tomotherapy System, Tomotherapy Inc., Madison, Wisconsin, USA), is an intensity modulated radiation therapy (IMRT) modality in which a 6 MV LINAC is mounted on a ring gantry that continuously rotates during the treatment. At the same time the couch is translated through the rotating beam plane so that the dose is delivered in a helical fashion. The beam intensity is modulated by a 64-leaf binary multileaf collimator (MLC). With this combination of MLC and table speed a highly conformal dose distribution can be achieved. The Tomotherapy system can acquire helical mega-voltage computed tomography (MVCT) images for daily image guidance using a lower energy (3.5 MV nominal) imaging beam, generated by the same LINAC that produces the therapeutic beam, coupled with an arc-shaped xenon detector array mounted on the rotating slip ring opposed to the radiation source [8,9]. After initial patient setup, a MVCT scan is acquired and fused with the planning computed tomography (kVCT) to determine couch adjustment, resulting in high precision positioning [10,11].

By means of helical tomotherapy it is possible to create treatment plans that deliver prescribed doses even in

regions close to the surface without the use of bolus [12–15]. For this reason helical tomotherapy has been used for treatments in which the skin is part of the PTV such as total scalp or whole breast irradiation [12,16]. Because of the high number of tangential fields in tomotherapy, dose to the skin could be higher than in fixed-gantry IMRT, as confirmed by measurements of dose to the skin *in vivo* [17]. In a study on nasopharyngeal cancer treated with helical tomotherapy, the side effects occurring more frequently were skin and mucosal reactions [18]. Therefore, given the importance of side effects to the skin in IMRT, accurate knowledge of dose to superficial structures is critical.

The reliability of planning system dose calculations at shallow depths is also a potential issue with intensity modulated treatments involving superficial structures. An overestimation of surface dose in phantom by the TPS of up to 14% has been reported for helical tomotherapy [13,14,16,19–22]. In a recent work, a significantly lower dose than TPS calculations was measured on a cheese phantom using optical stimulated luminescence (OSL) dosimeter, Si diodes, MOSFETs, and radiochromic films [23]. Several studies *in vivo* have also demonstrated that the TPS overestimate skin dose in tomotherapy treatments [13,24,25].

Dosimeters that have been used to evaluate superficial doses *in vivo* and in phantom for IMRT and tomotherapy include TLDs [15,26], diodes [27], and MOSFETs [14,22,24,26]. Radiochromic EBT films (International Specialty Products, Wayne, NJ) have many attractive characteristics that make them candidates for *in vivo* skin dosimetry such as high spatial resolution, near-tissue equivalence, and weak energy response [28–31]. Moreover, the equivalent depth in water of the effective point of measurement for EBT radiochromic films has been determined as 153 μm [29] which is very close to the clinically relevant depth for skin of 70 μm recommended by ICRP [32] and ICRU [33]. *In vivo* measurements of dose to the skin in helical tomotherapy have been performed using TLDs [13,15,24,25,34], and MOSFETs [24,25]. To our knowledge, radiochromic films have been used only for measurements of surface dose in phantom [20,21,23].

In this study we measured skin dose using radiochromic films *in vivo* on patients undergoing helical tomotherapy treatments with the Hi-Art Tomotherapy System treated for different pathologies, including treatments of head and neck, cranio-spinal axis (CSA), and inferior limbs. Skin dosimetry was aimed at checking delivered dose to the skin, in particular when an acute skin reaction had occurred. The aim of this study is to report the results of *in vivo* measurements, investigate factors possibly related to discrepancies between planned and measured dose, and study the dependence of EBT film response on the calibration method and on temperature at the time of irradiation.

Materials and methods

Film acquisition

In film handling and storing the recommendations of the AAPM TG-55 report [35] were followed: we used gloves to avoid film soiling; minimized exposure to light and kept films together to avoid differences in thermal histories. In the present study we used films from the same batch (# 36348-021). We scanned films with an Epson Expression 1680 Pro flatbed scanner (Seiko Epson Corporation, Nagano, Japan) [36]. The scanner was initialized by acquiring 5 blank scans and waiting 30 min warm-up time. A consistent orientation for films was maintained for all scans. Films were scanned at least 24 h after exposure. The central area of the scanner ($10 \times 15 \text{ cm}^2$) was used for film reading in order to minimize the non-uniform response of the scanner. The remaining area of the glass tray was covered by opaque radiographic films to reduce scattered light. The films were scanned in the 48-bit RGB transmission mode at 300 dpi resolution with all filter and image correction options turned off. The images were saved in a tagged image file format (TIFF).

Film analysis

The scanning of films and analysis of images were performed according to the protocol by Devic et al. [37]. Film images were analyzed with an in-house routine written with MatLab (The Mathworks, Inc, Natick, MA). For each exposed film we acquired five consecutive scans, calculated the average scan and applied a 2D Wiener filter in order to decrease image noise. The red component of each image was extracted to enhance film response. Pixels with a defective response because of the presence of specks or dust on the light pathway from the lamp to the CCD detector [37] were identified and removed from the analysis. In order to identify these pixels we acquired blank scans of the empty scanner bed taken over the same scanning region as the previously acquired images. Faulty pixels were identified as the pixels that differ by more than 5% from the maximum signal (2^{16}) in the blank image. The background signal of the scanner was determined by scanning a stack of three opaque radiographic films, providing as a result a dark image. We calculated the net optical density at a given dose D , netOD (D), from exposed, unexposed and dark images following Devic et al. [37], as:

$$\text{netOD}(D) = \log_{10} \left(\frac{I_{\text{unexp}} - I_{\text{bckg}}}{I_{\text{exp}}(D) - I_{\text{bckg}}} \right) \quad (1)$$

where I_{unexp} , and $I_{\text{exp}}(D)$, are the readings for unexposed and exposed film, while I_{bckg} is the reading from the dark image.

The uncertainty of dose was computed from the standard deviations of measured netOD and of parameters of the calibration function following the method from Devic et al. [37].

Film calibration

A calibration curve with EBT films was acquired at the TomoTherapy Hi-Art System following the procedure for

calibration recommended by Tomotherapy Inc. for delivery quality assurance (DQA) of treatments. Pieces of $3 \times 3 \text{ cm}^2$ films were exposed to a $10 \times 5 \text{ cm}^2$ static field in a solid water phantom (Tomo Solid Water Set, Standard Imaging Inc., Middleton, WI) at 1 cm depth, 85 cm SSD. Calibration doses ranged between 20 and 560 cGy. The condition of full backscatter was guaranteed by placing a 10 cm thick piece of solid water under the film. Dose to the films were reconstructed from measurements performed with an A15I Exradin thimble ion chamber placed at 1.5 depth. The average netOD was read inside a $5 \times 5 \text{ mm}^2$ ROI centred on each exposed film. The calibration function, in terms of dose versus netOD, was fitted with the following formula [37]:

$$D = b \cdot \text{netOD} + c \cdot \text{netOD}^n \quad (2)$$

where b , c and n are the parameters determined in the fitting process and D is the dose given to the film. The asymptotic 95% confidence intervals (CIs) for the estimated parameters and 95% prediction intervals for the fitted function were evaluated, assuming the asymptotic normal distribution for the parameter estimates, from the Jacobian matrix and the residuals of fit [38].

Dependence of response on the calibration method

We acquired a calibration curve by irradiating films with a helical treatment. A tomotherapy treatment was planned on a uniform cylindrical phantom, i.e. the Cheese Phantom (Standard Imaging Inc., Middleton, WI), specifically designed for the DQA of tomotherapy treatments. The treatment plan was designed to deliver different uniform doses to the regions of interest inside the phantom. Each target volume was cylindrical-shaped and encompassed the central coronal plane of the phantom. The treatment was delivered with EBT films inserted in the central coronal plane of the phantom, and was repeated, after removal of films, with A15I Exradin thimble ion chambers inserted into the target volumes. The doses to the films were 70, 105, 147, 200, 250, 300, 350 and 420 cGy. The calibration curve was calculated and compared with that obtained from a static beam. We then calculated the difference in dose between the two calibration curves, and the uncertainty on dose difference by summing in quadrature the CIs on the two calibration curves.

Dependence of film response on temperature

In order to verify the change in film response with temperature at the time of irradiation pieces of radiochromic film with size $1.5 \times 1.5 \text{ cm}^2$ were taped to the surface of a small solid water cube. The phantom was immersed in a thermostatic bath so that only its upper face, on which the radiochromic film was attached, was above the water level. The film piece was exposed to a $15 \times 15 \text{ cm}^2$ 6 MV beam produced by a Varian Clinac Trilogy (Varian, Palo Alto, CA) LINAC at an SSD of 140 cm and high dose rate. The treatment resulted in a total dose to the film of 3.4 Gy and the irradiation time was 3.3 min. The irradiation was performed with the water and the solid phantom at room temperature (22°).

Another EBT film was irradiated with the water temperature adjusted to keep the phantom surface at 34 °C, and with a lower dose rate, so that the irradiation lasted 20 min which is the maximum duration of a Tomotherapy treatment at our institute. For each phantom's temperature 5 films were exposed and the relative netODs were calculated and converted to dose.

In vivo measurements

Skin dose verifications with radiochromic films were performed on 14 patients treated with the Hi-Art Helical Tomotherapy System. The treated volumes were scalp (2), brain (1), head and neck (7), crano-spinal axis (CSA) (2) and inferior limbs (2). Patients were scanned with a GE Lightspeed QX/i CT scanner (GE Healthcare, Milwaukee, WI) with a 3.75 mm slice and 512 × 512 grid (0.99 mm/pixel) which was down-sampled to a 256 × 256 matrix upon import to the TPS [9] resulting in imported voxels of 1.98 × 1.98 × 3.75 mm³.

Five head and neck patients with metallic implants were scanned on the Tomotherapy MVCT since metallic implants cause fewer image artifacts in MVCT images compared to standard kVCT images [9]. The images set had 256 × 256 pixels of size 1.5 × 1.5 mm² and slice width 4 mm. The treatments were planned with the tomotherapy planning software. Dose was calculated in normal grid mode which results in dose calculations for every 2 × 2 imported CT voxels in the axial image [9]. The prescribed dose per fraction ranged from 180 to 400 cGy. One of the patients experienced grade 3–4 radiation dermatitis (See Fig. 1). The patients were immobilized and positioned before treatment by aligning fiducials to the red movable setup lasers in the treatment room. Three external fiducials per patient were used for setup, which consisted of skin tattoos for lower limb patients, and markings on masks for scalp,



Figure 1 Skin dosimetry with radiochromic films on a patient with acute skin reaction of grade 3–4.

brain, head and neck and crano-spinal axis patients. For all the patients in the study, MVCT images were acquired and fused with the planning image set for image guidance of the treatment. Image registration was at first performed automatically using a mutual information algorithm and then checked and adjusted manually if necessary before treatment. Positioning corrections were applied by automatic couch shifts in the longitudinal and vertical directions, manual couch shifts in the lateral direction, and roll rotations by automatic adjustment of the treatment angles.

Pieces of radiochromic film were applied to the patient's skin or to the inner side of thermoplastic mask used for immobilization. The dimensions of the film pieces varied from 1 × 1 to 1.5 × 1.5 cm². The films were applied to anatomical regions of interest for the radiation treatment; typical film positions were in correspondence to laser reference marks or anatomical markers. For some patients, the *in vivo* measurements were carried out over multiple treatment sessions. A total of 96 measurements were acquired. Measured doses were compared to dose to the skin on the treatment plan computed by the tomotherapy TPS. For every measurement we collected a set of values of planned doses to the skin in the voxels of the MVCT or KVCT which contained the radiochromic film. We recorded the midrange of these values and assumed it as planned skin dose. We also recorded the range of planned doses in the region of measurement. Table 1 shows, for each patient and region of interest, the planned dose, the range of planned dose values, and the number of repeated measurements over multiple fractions.

Results

The calibration curves of EBT films irradiated with a static beam and with a rotational beam are shown in Fig. 2. The 95% CI of the dose difference between the calibration functions obtained with the two methods included zero therefore the difference was not significant. The average dose on the films irradiated at $T = 22$ °C was 321.8 ± 12.0 cGy (1SD) while for the films exposed at $T = 34$ °C the average dose was 316.8 ± 13.9 cGy (1SD). Therefore the difference was within one standard deviation of measurements.

Table 1 and Fig. 3 show the results of *in vivo* measurements, their location on the patients and the percentage difference from dose calculated by the TPS. When measurements were performed only in one section of a treatment, the uncertainty in absorbed dose to the film as computed from the standard deviation of measured netOD and of parameters of the calibration function [37] is shown. When measurements were repeated for more than one treatment fraction on the same patient and location, the mean ± standard deviation of results over the repeated measurements is reported. Calculated and measured surface doses were linearly correlated (Pearson linear correlation coefficient 0.98).

The mean difference and standard error of the mean difference between measured and TPS-calculated dose was $-9.2\% \pm 2.6\%$ for all treatments. The mean absolute difference and its standard error were $10.2\% \pm 2.4\%$. For head and neck treatments, the mean difference was

Table 1 Results of skin dose verifications in patients treated with helical tomotherapy. When measurements are repeated for the same patient and anatomical site during radiotherapy, the average measured dose and its standard deviation is reported. When only one measurement was performed for a patient, the uncertainty is calculated from uncertainty on measured netOD following the method from Devic et al. [37]. The last column of the table lists the percent differences between measured and calculated dose defined as (measured – calculated)/calculated dose.

Patient no.	Site of treatment	Region of interest no.	TPS dose (cGy)	TPS dose range %	No. of measurements with EBT	EBT dose (cGy)	Difference EBT – TPS %
1	H&N	1	394	2.1	1	405 ± 14	2.8
2	H&N	1	92	39.1	11	93 ± 7	1.1
2	H&N	2	132	3.1	11	129 ± 8	-2.3
3	H&N	1	54.5	27.5	9	42 ± 4	-22.9
4	H&N	1	207	19.3	1	179 ± 9	-13.5
4	H&N	2	212	14.2	1	202 ± 10	-4.7
5	H&N	1	164	26.8	7	164 ± 8	0.0
6	H&N	1	129.5	8.5	8	124 ± 9	-4.2
6	H&N	2	127	10.2	8	120 ± 11	-5.5
7	H&N	1	13.5	7.4	4	12 ± 1	-11.1
7	H&N	2	153.5	3.3	1	134 ± 11	-12.7
8	brain	1	271	1.5	1	287 ± 18	-5.9
9	scalp	1	226	6.2	1	212 ± 8	-6.2
9	scalp	2	214	5.6	2	214 ± 11	0.0
10	scalp	1	158	3.2	4	147 ± 4	-7.0
11	CSA	1	86.5	54.3	3	81 ± 10	-6.4
12	CSA	1	146.5	4.8	5	112 ± 10	-23.5
12	CSA	2	40.5	49.0	2	37 ± 4	-8.6
13	lower limb	1	183	5.5	7	124 ± 7	-32.2
14	lower limb	1	179.5	5.0	9	120 ± 13	-33.1

$-6.6\% \pm 2.6\%$ and the mean absolute difference was $7.4\% \pm 2.3\%$. All these differences were statistically significant at the 0.05 significance level (*t*-Student test).

The difference between measured and calculated surface dose was not influenced by the presence of

a thermoplastic mask (Mann–Whitney *u*-test $p = 0.61$). Two measurements *in vivo* were performed on a patient who experienced acute side effects to the skin (patient no. 4 in Table 1). For these measurements the differences from the calculated doses were -13.5% and -4.7% .

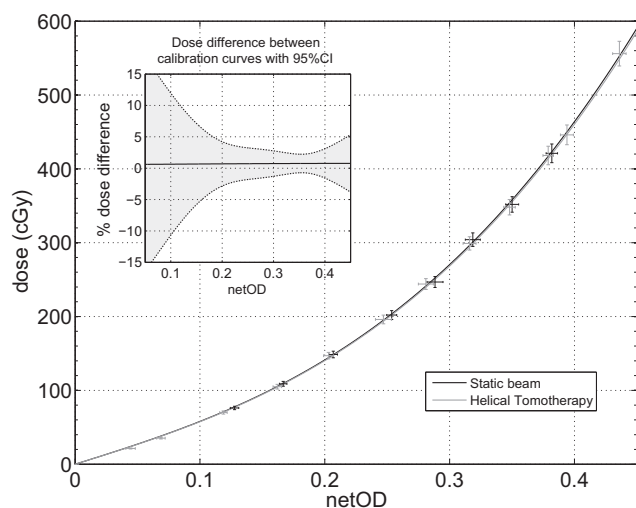


Figure 2 Calibration curves of radiochromic films acquired with static field (red) and helical tomotherapy (blue) in terms of dose versus net optical density (netOD). Error bars indicate 95% CIs for measured values of netOD and dose. The 95% CIs on calibration doses were assumed as 3.0% [45]. Uncertainties on netOD were estimated for each scanned film following the method from Devic et al. [37].

Discussion

Radiochromic films are usually calibrated with a static beam perpendicular to film surface. The arrangement of beams is completely different in a typical tomotherapy

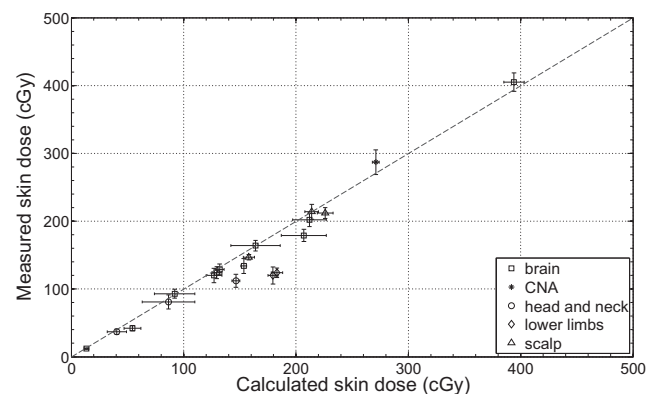


Figure 3 Skin doses measured with EBT films compared with doses calculated by the helical tomotherapy TPS, after averaging results over repeated measurements on the same patients and anatomical sites.

treatment, where radiation is delivered over 360° . Some authors reported a maximum increase in response of radiochromic films of 10% when the incident beam is parallel to the film [39]. Therefore the change in film response with the calibration method was quantified before using EBT films for *in vivo* skin dosimetry. Given that film response was independent from the method for calibration (Fig. 2), the simpler and faster static beam calibration method can be used to determine the calibration curve.

Another concern with *in vivo* use of radiochromic films is dependence on temperature at the time of irradiation. Films are usually calibrated at room temperature ($T \approx 22^\circ$) and, for *in vivo* measurements, are irradiated attached to the patient's skin ($T \approx 34^\circ$) for the duration of a treatment that can last for up to 20 min. In intra-operative radiotherapy, a correction of 0.95 to *in vivo* dose measured with radiochromic MD-55 films was introduced to account for temperature dependence [40]. We measured the dependence of dose reading on this change of temperature and irradiation time for EBT radiochromic films. The test revealed no significant dependence in film response. As a consequence no correction factor for temperature was applied to results of *in vivo* measurements.

Results of radiochromic film measurements show that the tomotherapy TPS dose algorithm overestimates superficial dose, in agreement with earlier findings *in vivo* and in phantom [13,14,16,19,20,22–25]. In particular, our results on head and neck patients are consistent with previous results of dosimetry of tomotherapy head and neck treatments on phantoms [13,14,19] and *in vivo* [13,22,24,25].

A reason for dose discrepancy is the difficulty of TPS to accurately calculate dose to the surface. In helical tomotherapy the dose calculation is performed using a convolution-superposition algorithm based on a collapsed cone approach [41,42]. Dose calculation inaccuracy at the air tissue interface in helical tomotherapy may originate from the assumed shape of the dose kernel near the surface in the TPS dose algorithms [43], or the inability of TPS to account for the contribution of contaminant electrons to the surface dose [44].

The helical tomotherapy TPS approximates each rotation as 51 equally spaced and discrete gantry angles. The discretization of the dynamic delivery may be a source of discrepancy of calculated to delivered dose, as in the actual delivery the dose from individual beamlets is dispersed over an arc that can span up to 7.1° . The dose blurring effect is more important for heavily weighted beams, because they have a longer opening time and therefore travel larger distances per gantry angle, and for beamlets that are located farther from the central axis. Therefore it could affect dose in the treatments of superficial targets, as beamlets near the surface are usually weighted more than deeper beamlets in order to achieve prescribed dose in the build-up region [43].

The limited accuracy of dose calculation at the surface could be caused by the finite size of the voxel in the patient CT scan. To each voxel at the surface is assigned one density value which is used to calculate dose, although it may contain air and tissue, two materials of extremely different density [14,23,24]. Spatial resolution of dose calculation is also critical [20], because with the Tomotherapy Hi-Art beam dose increases very rapidly within the

first millimeter of water [44]. In order to reduce the time needed for dose calculation and planning of treatment, in our patients the dose was calculated using a "normal" resolution grid, resulting in voxels of size $3 \times 3 \times 4 \text{ mm}^3$ for patients scanned with MVCT, and $3.96 \times 3.96 \times 3.75 \text{ mm}^3$ for patients planned on kVCT. These resolution grids are inadequate to accurately calculate dose in the build-up region. A "fine" calculation mode is available in the helical tomotherapy planning system, which results in a dose calculation grid that equals the imported CT data grid [9]. The usage of a fine resolution grid has been shown to improve the accuracy of calculated dose to the surface [20]. *In vivo* measurements with radiochromic films can also provide valuable skin dose information, as they have an effective point of measurement near to the clinically relevant depth for skin dose assessments of $70 \mu\text{m}$ [29].

The highest percentage differences between measured and calculated doses were found in treatments of lower limbs (-32% and -33% average). In order to find the reasons of these discrepancies, we investigated whether a change in patient anatomy occurred in the course of the radiotherapy treatment of the patient. By using the Tomotherapy Planned Adaptive software (HI-ART[®] version 3.1.5.3) we verified that no change in patient anatomy was observed around the point of measurement.

It has been hypothesized that in Tomotherapy treatments the discrepancy between planned and measured superficial dose is larger when more normally incident beams are used, because the dose gradient is greater in this scenario compared with obliquely incident beams [21]. In planning tomotherapy treatments of the lower limbs, directional blocking was applied to the contralateral leg in order to limit the dose to the healthy tissue. When directional block is applied to a structure the primary beamlets are not allowed to enter if the directionally blocked structure lies proximal to the target volumes. Therefore presumably inferior limb plans used more normally incident beams on the patient surface than other treatments and this could explain the high difference between measured and calculated dose.

One of the patients in this study experienced a side effect to the skin. In this case it was particularly important to check delivered dose to the skin, and measurements of skin dose *in vivo* were performed on the region in which the dermatitis occurred. Measured dose was lower than planned dose of -13.5% , a result that was well within the range of results obtained on other patients. Therefore we were assured that no error in treatment delivery had occurred which could cause an increase of dose to the skin. Re-optimization of the plan with stricter limits to superficial structures was then considered in order to further decrease the dose to the skin in the remaining fractions of the treatment.

Conclusions

Radiochromic EBT films are suitable detectors for surface dose measurements in tomotherapy treatments. The procedure of *in vivo* measurements with EBT films was relatively easy, and the time needed to setup for the *in vivo* measurements did not increase the overall treatment time. Results from *in vivo* measurements with EBT films confirm

that Helical Tomotherapy TPS overestimates dose in the build-up region. *In vivo* skin measurements with EBT films are a useful tool for quality assurance of tomotherapy treatments, as they can provide a quantification of dose in areas where the treatment planning system may not be accurate. This is of particular importance when the patient's surface is part of the target or is the dose-limiting organ at risk of the radiotherapy treatment, or when toxicity to superficial structures occurs to the patient during the treatment.

References

- [1] Lu JJ, Brady LW, Abitbol AA. Radiation oncology: an evidence-based approach. Berlin: Springer; 2008.
- [2] Archambeau JO, Pezner R, Wasserman T. Pathophysiology of irradiated skin and breast. *Int J Radiat Oncol Biol Phys* 1995; 31:1171–85.
- [3] Laskar S, Bahl G, Muckaden M, Pai SK, Gupta T, Banavali S, et al. Nasopharyngeal carcinoma in children: comparison of conventional and intensity-modulated radiotherapy. *Int J Radiat Oncol Biol Phys* 2008;72:728–36.
- [4] Rosenthal DI, Chambers MS, Fuller CD, Rebueno NC, Garcia J, Kies MS, et al. Beam path toxicities to non-target structures during intensity-modulated radiation therapy for head and neck cancer. *Int J Radiat Oncol Biol Phys* 2008;72:747–55.
- [5] Lee N, Chuang C, Quivey JM, Phillips TL, Akazawa P, Verhey LJ, et al. Skin toxicity due to intensity-modulated radiotherapy for head-and-neck carcinoma. *Int J Radiat Oncol Biol Phys* 2002;53:630–7.
- [6] Daly ME, Le QT, Maxim PG, Loo Jr BW, Kaplan MJ, Fischbein NJ, et al. Intensity-modulated radiotherapy in the treatment of oropharyngeal cancer: clinical outcomes and patterns of failure. *Int J Radiat Oncol Biol Phys*; 2009.
- [7] Thomas SJ, Hoole AC. The effect of optimization on surface dose in intensity modulated radiotherapy (IMRT). *Phys Med Biol* 2004;49:4919–28.
- [8] Mackie TR, Balog J, Ruchala K, Shepard D, Aldridge S, Fitchard E, et al. Tomotherapy. *Semin Radiat Oncol* 1999;9: 108–17.
- [9] Langen KM, Papanikolaou N, Balog J, Crilly R, Followill D, Goddu SM, et al. QA for helical tomotherapy: report of the AAPM task group 148. *Med Phys* 2010;37:4817–53.
- [10] Boswell S, Tome W, Jeraj R, Jaradat H, Mackie TR. Automatic registration of megavoltage to kilovoltage CT images in helical tomotherapy: an evaluation of the setup verification process for the special case of a rigid head phantom. *Med Phys* 2006; 33:4395–404.
- [11] Zhou J, Uhl B, Dewit K, Young M, Taylor B, Fei DY, et al. Analysis of daily setup variation with tomotherapy megavoltage computed tomography. *Med Dosim* 2010;35:31–7.
- [12] Orton N, Jaradat H, Welsh J, Tome W. Total scalp irradiation using helical tomotherapy. *Med Dosim* 2005;30:162–8.
- [13] Tournel K, Verellen D, Duchateau M, Fierens Y, Linthout N, Reynders T, et al. An assessment of the use of skin flashes in helical tomotherapy using phantom and *in-vivo* dosimetry. *Radiother Oncol* 2007;84:34–9.
- [14] Ramsey CR, Seibert RM, Robison B, Mitchell M. Helical tomotherapy superficial dose measurements. *Med Phys* 2007;34: 3286–93.
- [15] Zibold F, Sterzing F, Sroka-Perez G, Schubert K, Wagenknecht K, Major G, et al. Surface dose in the treatment of breast cancer with helical tomotherapy. *Strahlenther Onkol* 2009;185:574–81.
- [16] Reynders T, Tournel K, De Coninck P, Heymann S, Vinh-Hung V, Van Parijs H, et al. Dosimetric assessment of static and helical TomoTherapy in the clinical implementation of breast cancer treatments. *Radiother Oncol* 2009;93:71–9.
- [17] Roland TF, Stathakis S, Ramer R, Papanikolaou N. Measurement and comparison of skin dose for prostate and head-and-neck patients treated on various IMRT delivery systems. *Appl Radiat Isot* 2008;66:1844–9.
- [18] Kodaira T, Tomita N, Tachibana H, Nakamura T, Nakahara R, Inokuchi H, et al. Aichi cancer center initial experience of intensity modulated radiation therapy for nasopharyngeal cancer using helical tomotherapy. *Int J Radiat Oncol Biol Phys* 2009;73:1129–34.
- [19] Higgins PD, Han EY, Yuan JL, Hui S, Lee CK. Evaluation of surface and superficial dose for head and neck treatments using conventional or intensity-modulated techniques. *Phys Med Biol* 2007;52:1135–46.
- [20] Hardcastle N, Soisson E, Metcalfe P, Rosenfeld AB, Tome WA. Dosimetric verification of helical tomotherapy for total scalp irradiation. *Med Phys* 2008;35:5061–8.
- [21] Goddu SM, Yaddanapudi S, Pechenaya OL, Chaudhari SR, Klein EE, Khullar D, et al. Dosimetric consequences of uncorrected setup errors in helical Tomotherapy treatments of breast-cancer patients. *Radiother Oncol* 2009;93: 64–70.
- [22] Qi ZY, Deng XW, Huang SM, Zhang L, He ZC, Li XA, et al. *In vivo* verification of superficial dose for head and neck treatments using intensity-modulated techniques. *Med Phys* 2009;36: 59–70.
- [23] Snir JA, Mosalaei H, Jordan K, Yartsev S. Surface dose measurement for helical tomotherapy. *Med Phys* 2011;38: 3104–7.
- [24] Cherpak A, Studinski RC, Cygler JE. MOSFET detectors in quality assurance of tomotherapy treatments. *Radiother Oncol* 2008;86:242–50.
- [25] Kinkhikar RA, Murthy V, Goel V, Tambe CM, Dhote DS, Deshpande DD. Skin dose measurements using MOSFET and TLD for head and neck patients treated with tomotherapy. *Appl Radiat Isot* 2009;67:1683–5.
- [26] Kinkhikar RA. Surface dose for five telecobalt machines, 6 MV photon beam from four linear accelerators and a Hi-Art Tomotherapy. *Technol Cancer Res Treat* 2008;7:381–4.
- [27] Higgins PD, Alaei P, Gerbi BJ, Dusenbery KE. *In vivo* diode dosimetry for routine quality assurance in IMRT. *Med Phys* 2003;30:3118–23.
- [28] Butson MJ, Cheung T, Yu PK. Weak energy dependence of EBT gafchromic film dose response in the 50 kVp–10 MVp X-ray range. *Appl Radiat Isot* 2006;64:60–2.
- [29] Devic S, Seuntjens J, Abdel-Rahman W, Evans M, Olivares M, Podgorsak EB, et al. Accurate skin dose measurements using radiochromic film in clinical applications. *Med Phys* 2006;33: 1116–24.
- [30] Bufacchi A, Carosi A, Adorante N, Delle Canne S, Malatesta T, Capparella R, et al. *In vivo* EBT radiochromic film dosimetry of electron beam for Total Skin Electron Therapy (TSET). *Phys Med* 2007;23:67–72.
- [31] Rink A, Vitkin IA, Jaffray DA. Energy dependence (75 kVp to 18 MV) of radiochromic films assessed using a real-time optical dosimeter. *Med Phys* 2007;34:458–63.
- [32] International Commission on Radiological Protection. 1990 recommendations of the International Commission on Radiological Protection. Pergamon for the Commission; 1991.
- [33] International Commission on Radiation Units and Measurements. Determination of dose equivalents resulting from external radiation sources: vol. 43, Part 2; 1985.
- [34] Ito S, Parker BC, Levine R, Sanders ME, Fontenot J, Gibbons J, et al. Verification of calculated skin doses in postmastectomy helical tomotherapy. *Int J Radiat Oncol Biol Phys*; 2011.
- [35] Niroomand-Rad A, Blackwell CR, Coursey BM, Gall KP, Galvin JM, McLaughlin WL, et al. Radiochromic film dosimetry:

- recommendations of AAPM radiation therapy Committee Task Group 55. *Med Phys* 1998;25:2093–115.
- [36] Paelinck L, De Neve W, De Wagter C. Precautions and strategies in using a commercial flatbed scanner for radiochromic film dosimetry. *Phys Med Biol* 2007;52:231–42.
- [37] Devic S, Seuntjens J, Sham E, Podgorsak EB, Schmidtlein CR, Kirov AS, et al. Precise radiochromic film dosimetry using a flat-bed document scanner. *Med Phys* 2005;32:2245–53.
- [38] Seber GAF, Wild CJ. Estimation methods. In: *Nonlinear regression*. Hoboken, NJ: John Wiley & Sons, Inc.; 1989. 2005, p. 21–89.
- [39] Suchowerska N, Hoban P, Butson M, Davison A, Metcalfe P. Directional dependence in film dosimetry: radiographic and radiochromic film. *Phys Med Biol* 2001;46:1391–7.
- [40] Ciocca M, Orecchia R, Garibaldi C, Rondi E, Luini A, Gatti G, et al. *In vivo* dosimetry using radiochromic films during intraoperative electron beam radiation therapy in early-stage breast cancer. *Radiother Oncol* 2003;69:285–9.
- [41] Sterpin E, Salvat F, Olivera G, Vynckier S. Monte Carlo evaluation of the convolution/superposition algorithm of Hi-Art tomotherapy in heterogeneous phantoms and clinical cases. *Med Phys* 2009;36:1566–75.
- [42] Lu W, Olivera GH, Chen ML, Reckwerdt PJ, Mackie TR. Accurate convolution/superposition for multi-resolution dose calculation using cumulative tabulated kernels. *Phys Med Biol* 2005;50:655–80.
- [43] Cheek D, Gibbons JP, Rosen II, Hogstrom KR. Accuracy of TomoTherapy treatments for superficial target volumes. *Med Phys* 2008;35:3565–73.
- [44] Smith KS, Gibbons JP, Gerbi BJ, Hogstrom KR. Measurement of superficial dose from a static tomotherapy beam. *Med Phys* 2008;35:769–74.
- [45] International Atomic Energy Agency. Absorbed dose determination in external beam radiotherapy: an international code of practice for dosimetry based on standards of absorbed dose to water. Vienna: International Atomic Energy Agency; 2000.